Chapter 4

Poly (vinylidene fluoride)/Nitrogen doped carbon dots nanocomposite film with improved storage properties for high energy density applications

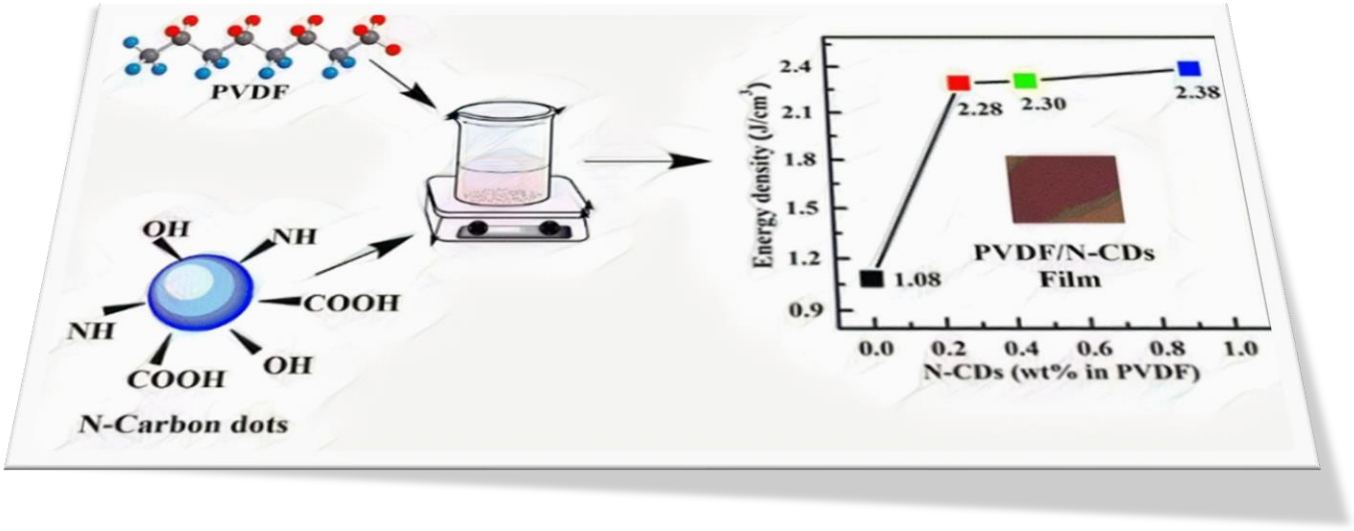

Chapter 4: Poly (vinylidene fluoride)/Nitrogen doped carbon dots nanocomposite film with improved storage properties for high energy density applications

6.1 Introduction

In Chapter 1, we have introduced about the existing literature on Poly (vinylidene fluoride) (PVDF) nanocomposite films investigated using various types of nanofillers. A comprehensive literature survey on the PVDF nanocomposites suggests that carbon-based nanofillers have received special attention. To improve the dielectric properties of PVDF, one dimensional filler like 'carbon nanotubes' (CNTs), and Graphene nanosheets (GNs) were used by various researcher [130,131]. Achaby et al. investigated graphene oxide (GO)/PVDF nanocomposite and showed that -C=O bond in GO helps in the formation of β-phase in PVDF [131,132]. The NH_2-treated graphene nanodots/reduced graphene oxide (RGO), has also improved the dielectric constant of the PVDF matrix by increasing content of ferroelectric β-phase[133]. The carbon-based nanomaterials have vast applications in bioimaging, electronic devices and drug delivery systems owing to their biocompatible physical and chemical properties less-toxicity[134,135]. Carbon dots have got attention due to their low cost synthesis, ability to host diverse elements on their surface and good biocompatibility[136]. The size of carbon dots and Nitrogen doped carbon dots (N-CDs), studied in earlier literature, is in the range of 2.5 to 5nm. The doping of Nitrogen in carbon dots induces delocalization and increase in charge transfer[137]. The N-CDs have various functional groups like C-N, C=N, C=O, COOH, -OH and C-O on its surface[135]. It is well established fact that the higher surface functionality of fillers in PVDF can help in the formation of electroactive phase of PVDF matrix, which may result in the enhancement of dielectric and ferroelectric properties[138].

In this Chapter, we report the results of our investigation on the synthesis and characterization of PVDF/N-CDs (PNC) based nanocomposite films, to exploit their

applications in the high-density capacitive energy storage, for the first time. The N-CDs were synthesized by the solvothermal process with the DMF as solvent. The PVDF/N-CDs nanocomposite films were prepared by solution cast method, using different concentrations of N-CD fillers viz. 0.0 (pure PVDF), 0.3, 0.5 and 1 weight % (wt.%), considering the fraction of the two components of the composite, weight by weight (w/w). The resulting compositions of the PVDF/N-CDs are now onwards denoted by PNC0.3, PNC0.5 and PNC1. A further higher concentration of the N-CD filler resulted into early breakdown of the nanocomposite due to formation of the conductive path because of the percolation effects, and therefore not considered in the present study. For a comparative study and reference, pure PVDF film was also prepared and characterized along with the different compositions of the developed nanocomposites. The structural, morphological, dielectric and ferroelectric properties of the developed nanocomposites were investigated using various characterization techniques elaborated in chapter 2. The dielectric breakdown strength of the developed nanocomposites was also estimated using Weibull analysis. Significant enhancements in the dielectric constant, energy storage density and energy discharge efficiency are obtained in the developed nanocomposite, and the results are discussed in details in subsequent sections.

6.2 Experimental

6.2.1 Synthesis of Nitrogen doped Carbon dots (N-CDs)

The synthesis of N-CDs was done following the standard solvothermal procedure reported in the earlier literature[139]. We took 0.42g (1 mmol) Citric Acid and 0.36 (3 mmol) urea and dissolved into 10 ml, Dimethylformamide (DMF) solvent, stirred until the solution became clear and transparent. This solution was transferred to 50 ml Teflon lined stainless autoclave and heated at 160℃ for 4 hours. The resulting product was centrifuged at 5000 rotation per minutes (rpm) for 5 minutes to get the N-CDs. A schematic diagram of the synthesis process is shown in Fig. 4.1 (a).

6.2.2 Synthesis of PVDF/N-CDs nanocomposite films

The synthesis of self-standing nanocomposite films of various compositions was done with the help of solution cast method as shown schematically in the Fig. 4.1(b). As per the amount required for a particular composition of PVDF/N-CDs, the N-CDs were dispersed in DMF for 2 hours at 1400 rpm using a magnetic stirrer hot plate followed by ultrasonication for 30 minutes. Simultaneously, at another hot plate, the PVDF was dissolved in DMF by stirring at 55°C. Homogeneously dispersed N-CDs in DMF solvent was poured in the PVDF solution and composite mixture was further heated at 55°C on magnetic stirrer at 10000 rpm for 7 hours. In the next step, the mixture was ultrasonicated for 10 minutes, and then poured in a petri dish to form a thin layer. It was subjected to drying in an oven at 120°C for 12 hours to get the self-supporting nanocomposite film of average thickness around 0.060 ±2 mm.

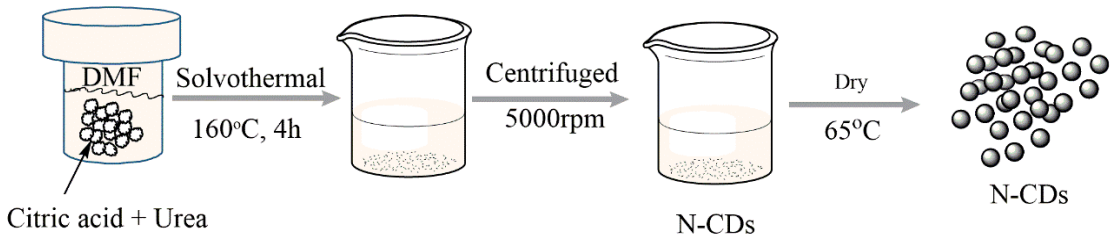

Fig. 4.1(a) Schematic diagram for synthesis process of Nitrogen doped carbon dots

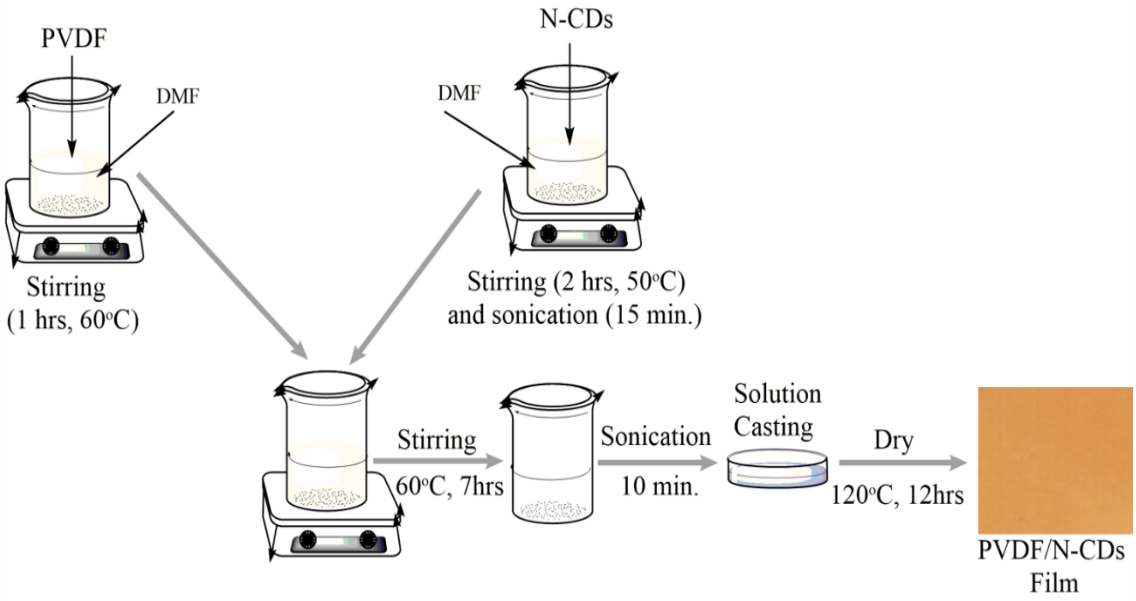

Figure 4.1(b) Schematic diagram for synthesis process of PVDF/N-CDs nanocomposite films

6.3 Result and Discussion

6.3.1 Characterization of N-CDs

The morphology of the as prepared N-CDs was characterized by the high-resolution transmission electron microscopy (HR-TEM) and the recorded microstructure is shown in Fig.4.2(a). The N-CDs can be seen as dark spots in this Fig. while the background corresponds to DMF solvent used as dispersing medium for mounting the sample on Cu-grid. The N-CDs are seen to have spherical and uniform shape with average diameter of 2.44 nm as depicted by the histogram shown in Fig. 4.2(b). The powder XRD pattern of NCDs shown in Fig. 4.2(c) exhibits a broad peak which shows that the N-CDs are having more amorphous carbon cluster [30,31]. The broad peak around 22.6° corresponds to average d-spacing around 0.366nm, for the N-CDs, which is higher than that expected for graphite (0.33nm). A weak overlapping broad peak around 26.7 may be attributed to the partial crystalline nature of N-CDs[136,140,141].

N-CDs were also characterized using FTIR spectroscopy and the spectrum is shown in Fig.4.2(d). Several peaks seen in the FTIR spectrum indicate the presence of various functional groups at the N-CDs surface. The doping of Nitrogen in carbon dots can be evidenced by the C-N stretching vibration seen at 1182 cm^{-1} [136,141,142]. The stretching vibration in the range 3160-

3640 cm^{-1} indicates the presence of O-H bond which is responsible for imparting hydrophilicity and high dispersibility in water. Further, the peaks seen at 1710 cm^{-1}; 2940 cm^{-1}; 1408 cm^{-1}; 1286 cm^{-1} and 1350 cm^{-1} correspond to the C=O; C-H; C-O and C-O-C stretching vibrations respectively. This suggests that surface of N-CDs is passivated with several surface functional groups[136,141–143].

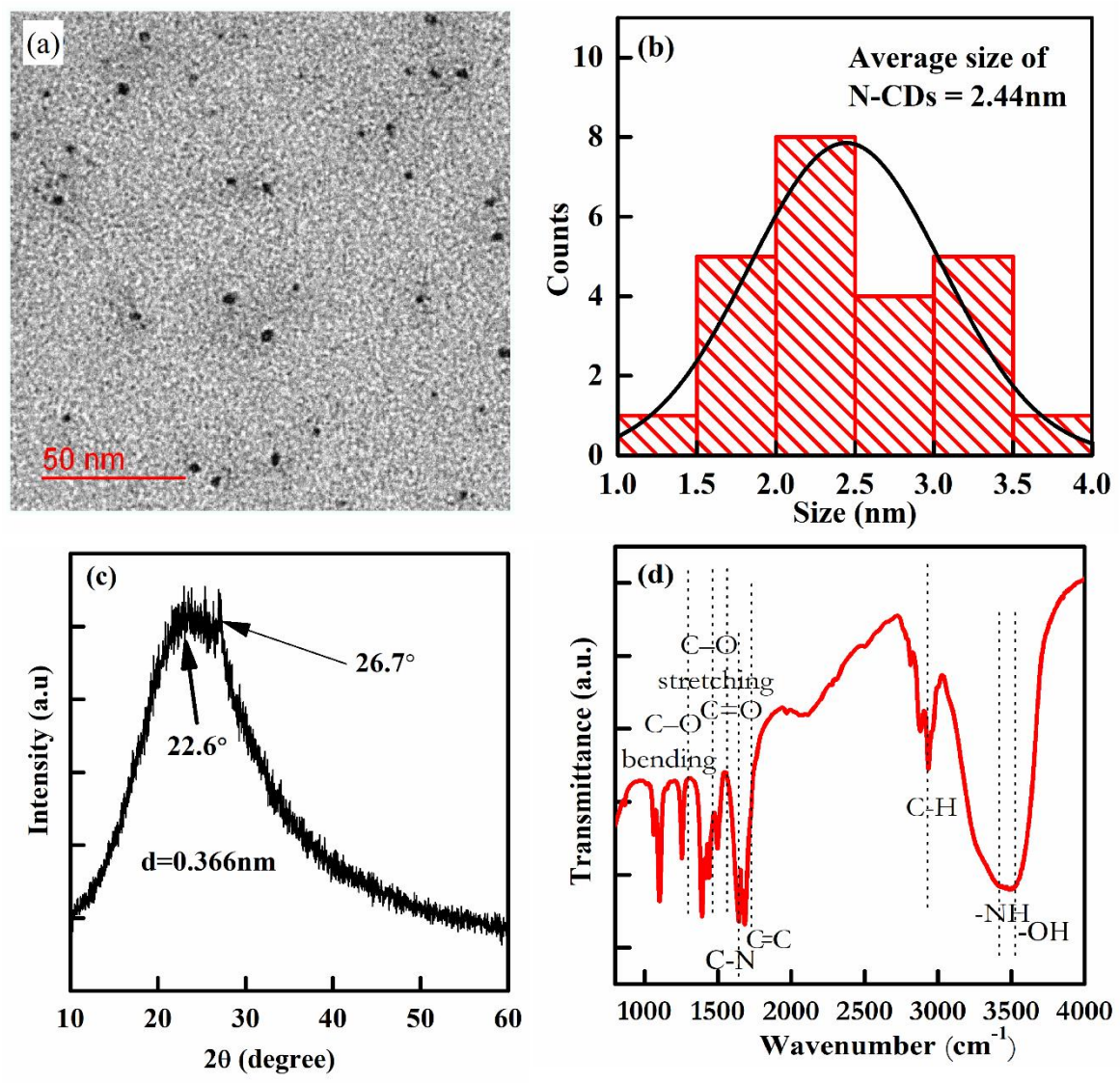

Figure 4.2 (a) HR-TEM images of N-CDs, (b) Showing the particle distribution of N-CDs, (c) XRD Pattern and (d) FTIR spectrum of N-CDs showing the functional groups.

The optical properties of N-CDs were studied with the help of UV-Vis spectroscopy and photoluminescence (PL) spectrum, as shown in Fig. 4.3 (a). There are three peaks in UV-

Vis spectra around 211nm, 345 nm and 450 nm. The 211 nm peak is ascribed to the π-π* transition of the aromatic C=C bond, the 345 nm peak is attributed to the n-π* transition of C=O and the broad peak around 450 nm may correspond to the presence of amino functionalized group attached to carbon dots confirming the doping of Nitrogen in Carbon dots[136,141]. The PL (photoluminescence) spectrum of N-CDs using excitation wavelength (λ_{ex}) of 375nm gives the emission peak at 450nm that is in the blue-green region[136].

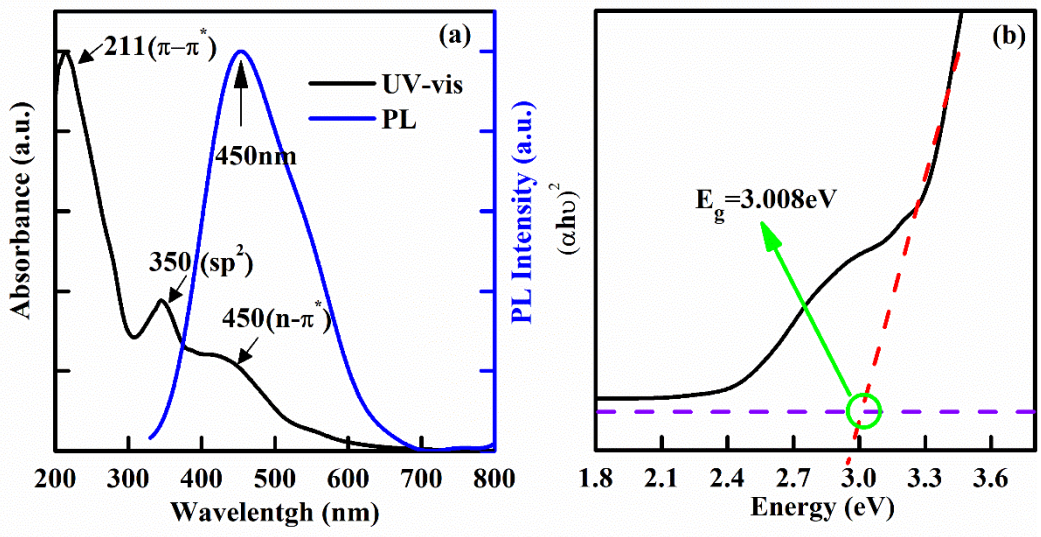

Figure 4.3 (a) UV-Vis spectrum, PL Spectra of N-CDs excited at a wavelength of 375nm, (b) Tauc plot ($(\alpha h\upsilon)^2$ vs $h\upsilon$).

The Tauc's plot ($(\alpha h\upsilon)^2$ vs. $h\upsilon$) is used to determine the band gap (E_g) of the direct band gap semiconductors, where α, h, υ are absorption coefficient, Planck's constant, and light frequency respectively. The calculated band gap for N-CDs is around 3.066eV, as shown in Fig. 4.3(b) by the extrapolated linear fit intercept at *hυ* (energy axis) in the Tauc plot[144].

6.3.2 Structural analysis PVDF/N-CDs with XRD, FTIR and DSC

To identify the polymorphic phases in PVDF/N-CDs nanocomposite films, XRD analysis and FTIR spectra measurements were performed. The XRD patterns of all the developed compositions of PVDF/N-CDs (PNC0.3%, PNC0.5% and PNC1%) nanocomposites are shown in Fig.4.4(a), along with that for pure PVDF film prepared in this work. The

monoclinic α-phase peak can be seen at 2θ angle of 26.5°(021), while γ-phase peaks are seen at 18.5°(020), 39.0°. The ferroelectric β-phase peaks are seen 20.6° (200/100 planes), 36.1° and 42.3° [6,145]. It can be seen form Fig.4.4(a) that, the crystalline β, γ-phases are dominating in all the compositions. The α-phase of pure PVDF is slightly suppressed after nanocomposite formation with N-CDs, as evidenced from inset to Fig.4.4(a). Thus, the XRD studies reveal that the ferroelectric polar phases are becoming the major phase after PNC nanocomposite formation.

The crystallinity of nanocomposite films was calculated using the XRD pattern of all the developed compositions. The crystallinity (χ_c) of nanocomposite can be calculated from the XRD pattern, using following equation:

$$\chi_C = \frac{\sum A_{cr}}{\sum A_{cr} + \sum A_{amr}} \times 100\% \quad (4.1)$$

Where, $\sum A_{cr}$, $\sum A_{amr}$ are the summation of the integral area of the crystalline and amorphous region peaks, respectively, in the XRD pattern[97,147].

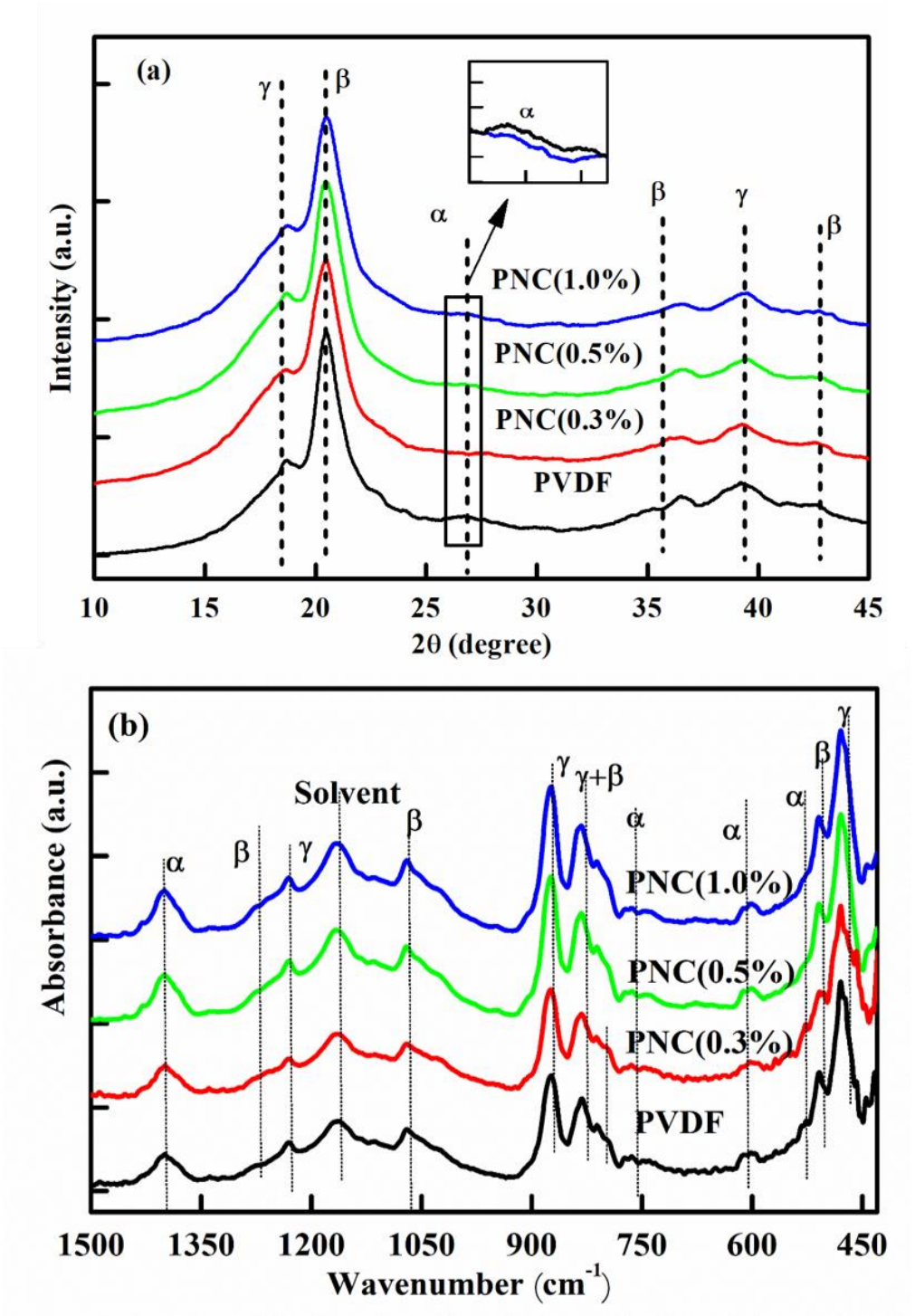

Figure 4.4 (a) XRD patterns and (b) FTIR spectra of PNC nanocomposite films with PVDF.

Further phase analysis of the prepared samples was carried out using FTIR data shown in Fig.4.4(b). The β-phase absorption peaks are seen at 510cm^{-1}, 1071cm^{-1}, 1274cm^{-1}. The absorption peaks at 473cm^{-1}, 840cm^{-1}, 876cm^{-1} and 1231cm^{-1} are attributed to the γ-phase. The α-phase peaks can be seen at 881cm^{-1}, 764cm^{-1}, 615cm^{-1}, 530cm^{-1} [6,100,145,146]. The strong

absorption at 1402cm^{-1} is corresponding to the stretching vibration of C-H bonds, while the band located at 1274cm^{-1} is attributed to the stretching vibration of C-F bonds[6,100,145]. The relative proportion of electroactive γ, β-phases can be calculated from the FTIR spectra with the help of the following equation:

$$F(\beta+\gamma) = \frac{A_{(\gamma+\beta)}}{\left(K_{(\gamma+\beta)}/K_{(\alpha)}\right)A_{\alpha} + A_{(\beta+\gamma)}} \quad (4.2)$$

Where, A_{α}, $A_{(\beta+\gamma)}$ represent the absorption intensity of the dominant peaks for these phases. The K_{α} and $K_{\beta+\gamma}$ are the corresponding absorption coefficients with the values 0.365 and 0.150 μ/m, respectively, as reported in earlier literature[97,147]. As reported in earlier literature,[97,147] in pure PVDF, the dominant absorption intensity peak corresponding to the 'α' phase appears at 764cm^{-1} while that for electroactive (β+γ) phases it appears at 832 cm^{-1}. However, in pure PVDF film prepared by us, the peak at 764cm^{-1} is rather weak, which suggests that even in pure PVDF the (β+γ) electroactive phases are sufficient in proportion in comparison to the nonpolar 'α' phase. After PNC nanocomposite formation, the relative proportion of electroactive phase (β+γ) has increased further with the increasing concentration of N-CDs filler loading as given in the table 4.1.

Table 4.1 Crystallinity and relative proportion of electroactive phases in the PVDF and the nanocomposites films

Sample	Crystallinity (XRD)	Proportion of electroactive phases (FTIR)
PVDF	39.89	73.33%
PVDF/N-CDs (0.3%)	43.09%	74.10%
PVDF/N-CDs (0.5%)	46.58%	76.88%
PVDF/N-CDs (1.0%)	56.52%	77.09%

Differential Scanning Calorimetry (DSC) was performed to characterize the developed nanocomposite and pure PVDF films. It is well known that coherence energy of the electroactive phases (β, γ-phases) is higher due to the stronger dipole interaction and therefore the endothermic melting temperature (T_m) for the α-phase is lower than the β, γ-phases.[97,146] The DSC plots for PNC0.3%, PNC0.5%, PNC1% and pure PVDF films are shown in Fig.4.5 The normalized DSC curve shows that the T_m for the pure PVDF is 167.05 ℃ which increases by 1 ℃ to 168.09 ℃ for PNC 1%. This 1 ℃ increment in T_m is due the increment in the proportion of the electroactive β, γ-phases. Minor or no difference in T_m is seen for PNC 0.3% and PNC 0.5 % due to lower amount of filler. In pure PVDF, at 161.6℃ extra endotherm melting can be seen which is representing the presence of premature melting of α-phase [97,146]. This premature melting peak disappears after nanocomposite formation with N-CDs.

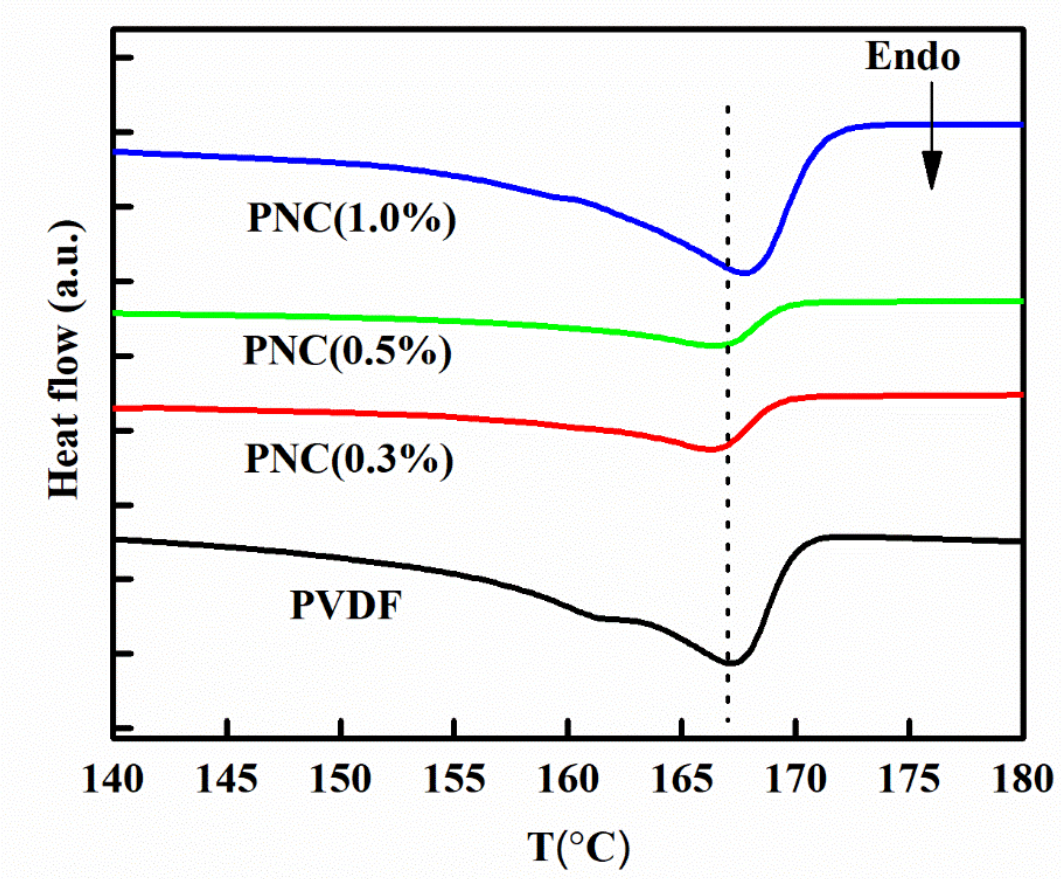

Figure 4.5 DSC plots for pure PVDF and PNC nanocomposite films.

The XRD, FTIR and DSC characterization of the developed nanocomposite films indicate the enhancement in the proportion of the crystalline and electroactive phases. The increased proportion of electroactive phase in the nanocomposite films as compared to pure PVDF, can be attributed to the interaction between the N-CDs and PVDF, which promotes the formation of the electroactive polar phase. This is illustrated in Fig.4.6 with the help of a schematic diagram. This enhancement in the electroactive phase fraction is the consequence of the interaction of -CF_2- of PVDF with the -NH- of the N-CDs while the delocalized π-electrons present in the N-CDs are having interaction with the -CH_2- dipoles of the PVDF. Attractive and repulsive interactions are assumed to take place between the -CH_2-, -CF_2- dipoles of PVDF and - NH- and delocalized π-electrons of N-CDs. Further, we may also say that N-CDs have -OH, carbonyl groups (functional groups) which can interact with the F and H atoms of the PVDF.

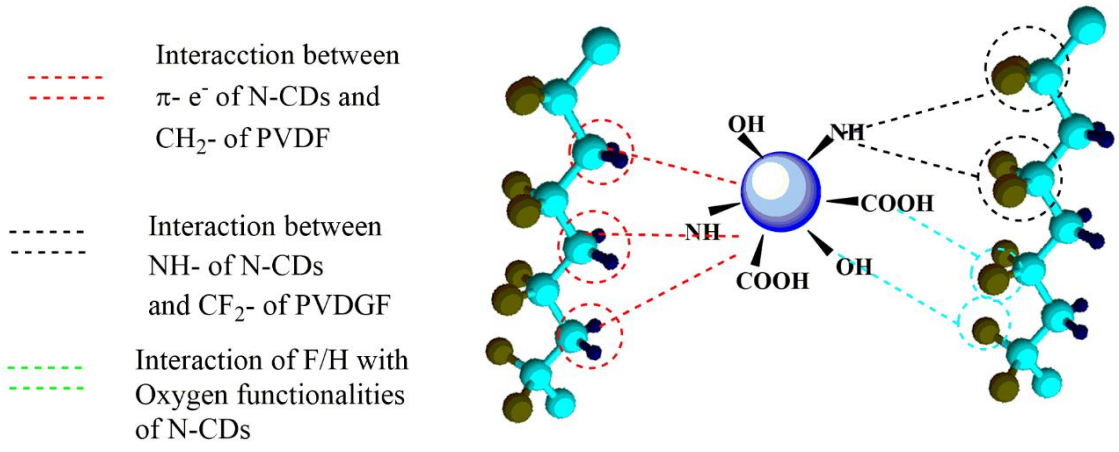

Figure 4.6 Schematic diagram of interaction between the PVDF matrix and loaded N-CDs fillers in the PNC nanocomposite films.

6.3.3 XPS Analysis of the PVDF/N-CDs Films

A comparative surface chemistry analysis of the PVDF and PNC (1%) was done with the help of XPS data survey as shown in Fig. 4.7 (a). We could not see any remarkable difference

between the XPS spectra survey of pure PVDF and PNCs film but minor peak shifts can be noticed. After nanocomposite formation, N-CDs add nitrogen as the extra element to the PVDF matrix but due to very low concentration of filler no clear peak representing the nitrogen can be seen in the XPS survey. For further verification, we have zoomed selected portion of the XPS spectra in the range of 390 eV to 400 eV as shown in Fig.4.7(b). Presence of the N1s peak that belongs to the -CN group can be clearly seen in this portion which further confirms the existence of N-CDs in the developed nanocomposite films[136,148,149]. The binding energy peak for F1s of the PNC is slightly shifted to the lower energy (687.45 eV) than that for the pure PVDF (687.75 eV) as can be seen from Fig.4.7 (c). This deviation in the binding energy can be ascribed to the intermolecular interactions between highly polarized backbone's ($–H^{\delta+}–C^{\delta+}–F^{\delta-}–$ dipoles) hydrogen atom of PVDF and π- orbitals of N-CDs.[104,148] Fig. 4.6 schematically shows this interaction. The zoom in portion of the XPS spectra for the C1s peak position in PVDF and PNC films shows three peaks. The two peaks at the binding energy 290.9 eV and 286.6 eV correspond to the $–CH_2$ and $–CF_2$ of the PVDF backbone, respectively, while the third shoulder peak at 284.6 eV, is related to the non-oxygenated carbon ($-C_xH_y-$). In PNC, the C1s peaks corresponding to $–CH_2$ and $–CF_2$ are shifted to the higher binding energy caused by the presence of oxygenated carbon. The presence of the oxygenated carbon in the PNC film proves the inclusion of the N-CDs [148].

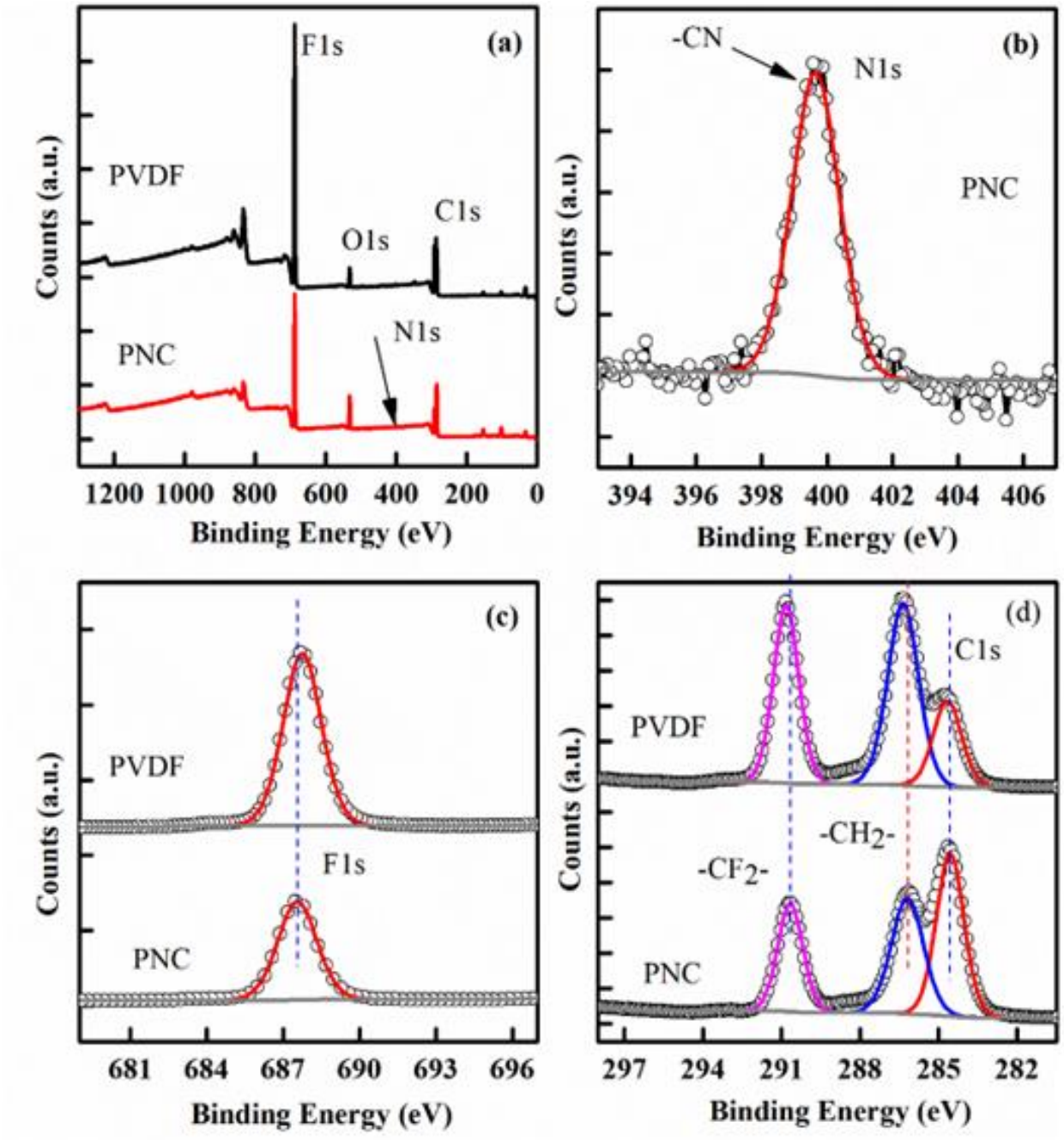

Figure 4.7 (a) XPS Survey of PVDF and PNC1%, (b) N1s peak of PNC (1%), (c) F1s peak of the PVDF and PNC (1%) and (d) C1s peak of the PVDF and PNC (1%).

6.3.4 AFM Micrographs analysis

The Fig. 4.8(a, b) shows the AFM images of the pure PVDF and PNC (1wt%) nanocomposite films. The PNC nanocomposite seems to have slightly low roughness, which could be due to smaller or invisible spherulite present in the nanocomposite film as compared

to the pure PVDF film. However, roughness profile measurement reveals that the two films have quite close roughness. This can also be understood by the smaller size of the spherulites as confirmed in FE-SEM micrographs. Another reason of higher roughness may be due to hydrophilic nature of the N-CDs during the fast exchange of the solvent and filler particles. Fig. 4.8(c, d) shows the AFM micrographs surface roughness profiles for pure PVDF and PNC1% films, respectively. The estimated root mean square roughness of the surface is 8.56±0.5 nm for PVDF film and 8.43±0.5 nm for PNC nanocomposite film. Thus, the roughness of the two films is comparable.

The power spectral density (PSD) describes how different spatial frequencies contribute to the surface structure, offering extra information about surface roughness. A thorough discussion of surface topography characterization using spectral analysis can be found elsewhere [150]. With the help of Nova Px 3.0.4 rev software, the isotropic PSD of the AFM image of pure PVDF and PNC1% nanocomposite was plotted. The PSD of the two films with Hann windowing are shown in the Fig. 4.8 (e). The isotropic PSD demonstrates that there is no preferential orientation of the surface features and that surface polymerization proceeds without a preferred growth direction. For charge storage applications, the isotropic polymer growth helps prevent charge leakage and hence increases charge storage endurance. If the charge storage rather than transport is the desired polymer functionality, a synthetic strategy that promotes isotropic polymer development is preferred [114,150].

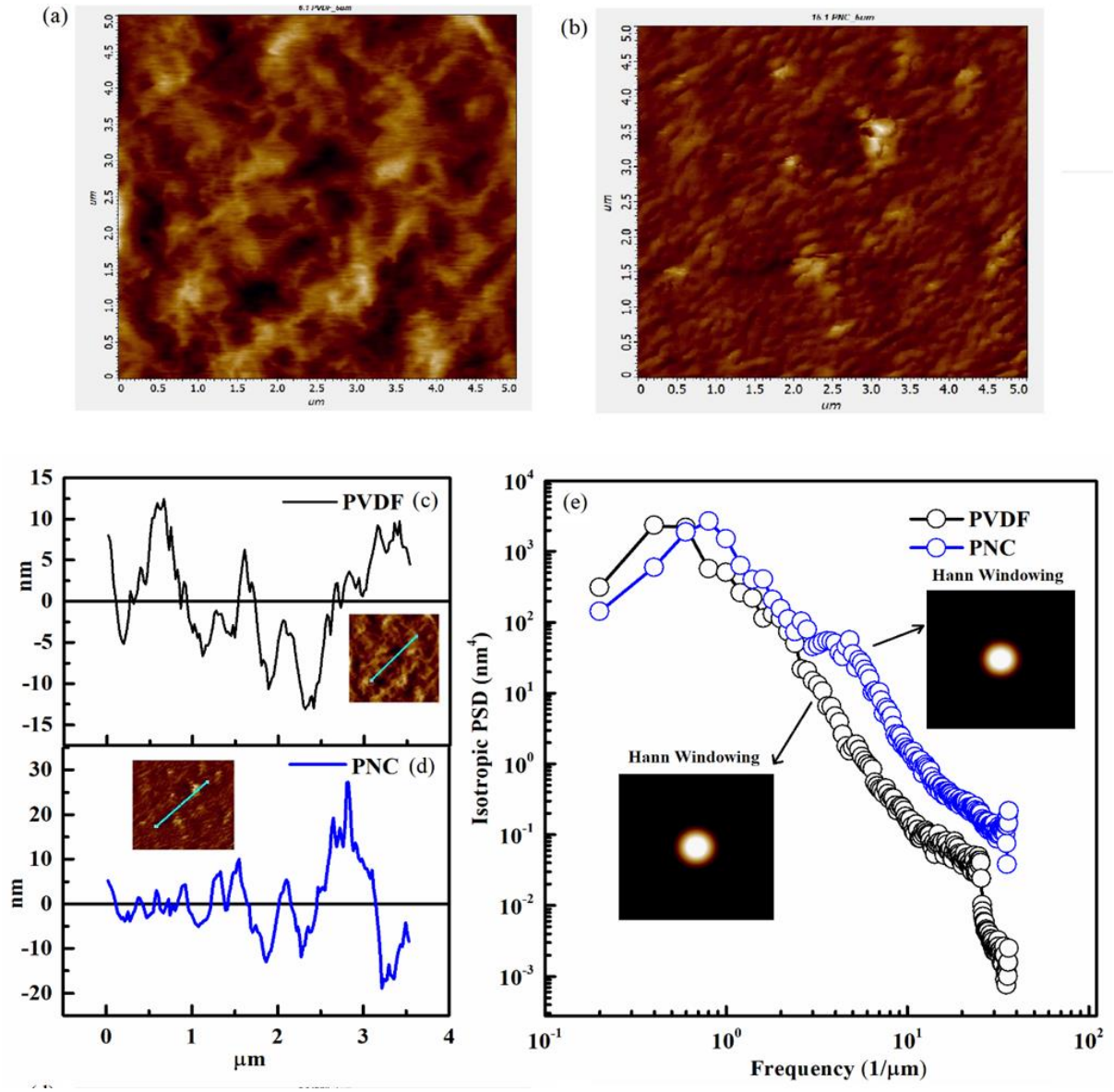

Figure 4.8 AFM Surface images of (a) PVDF and (b) PNC (1%); Roughness profile of (c) pure PVDF and (d) PNC (1%); Isotropic 2D PSD plot and Hann Windowing of AFM micrographs for pure PVDF and PNC (1%) (c).

6.3.5 Morphological analysis

Figs.4.9 (a), (b), (c) and (d) show the FE-SEM micrographs of pure PVDF, PNC (0.3%), (0.5%), (1%) films, respectively. The element mapping for PNC (1wt%) is also shown in Fig.4.9(e). The spherulitic microstructure characteristics can be clearly seen in the micrographs of pure PVDF and PNC films upto 0.5% of N-CDs. It is well known in polymers that crystallization is slow process, as it requires formation of nuclei and growth of crystals for

bigger molecules. The spherulite size in pure PVDF film is having average size around ~13 µm, as can be seen in Fig. 4.9(a). It is evidenced from Fig. 4.9(b, c) that, the average size of spherulites is decreased as the concentration of N-CDs is increased to 0.3% and 0.5%, in PNC nanocomposites. The nanofiller act as nucleating sites that increases the speed of nucleation more than that of grain growth. The grain growth is obstructed by the large loading of nanofiller, and the resulting spherulite size become smaller [111,151]. The larger number of spherulites are forming in the presence of N-CDs due to accelerated crystallization process via heterogeneous nucleation [151]. Further, when the N-CDs concentration is increased to 1% in PVDF, the spherulites become very small in size and difficult to resolve clearly. The PNC 1% film thus evolves with smoother surface as shown in Fig. 4.9(d). The densification and orderly arrangement of crystalline grain type smaller spherulites array could have resulted in smoother surface[97]. With the help of elemental mapping, we can see the presence of nitrogen group (-NH) in the film which is the evidence of the N-CDs in nanocomposite films.

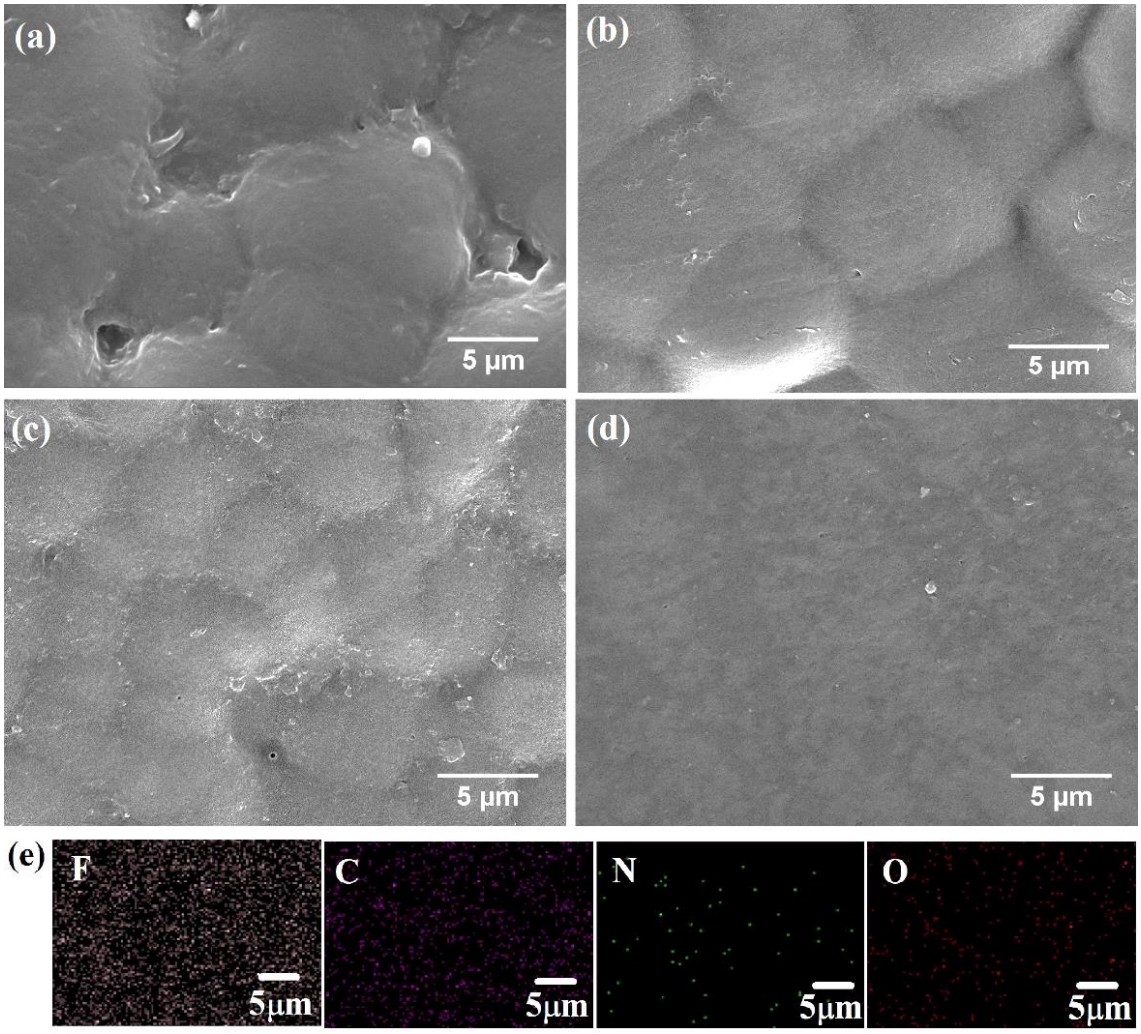

Figure 4.9 FE-SEM micrographs of (a) PVDF, (b) PVDF/N-CDs (0.3%), (c) PVDF/N-CDs (0.5%), (d) PVDF/N-CDs (1%), (e) Element mapping showing the presence of N-CDs in PNC (1%) nanocomposite.

6.3.6 Dielectric properties of PVDF/N-CDs nanocomposite films

The dielectric properties of PNC nanocomposites were investigated for the capacitive energy storage applications. The dielectric permittivity and loss are important parameters to determine the charge holding capacity, power recovered and loss over each cycle of charging/discharging. Fig. 4.10 shows the temperature dependence of (a) dielectric constant, (b) dielectric loss (tanδ) for various compositions of PNC nanocomposite films measured at 1kHz. As can be seen from Fig.4.10, the dielectric response for pure PVDF film prepared in the present work is consistent with previous reports[40].

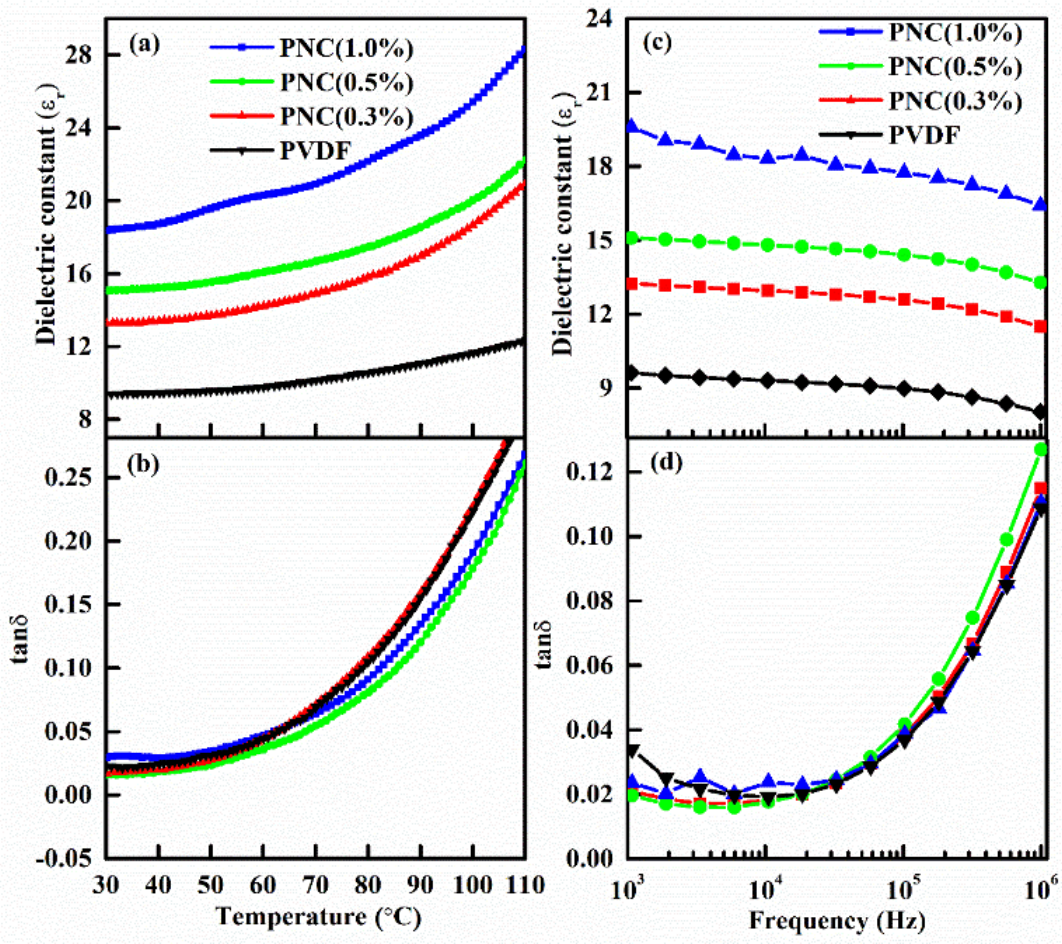

Figure 4.10 Temperature dependence of (a) dielectric constant, (b) dielectric loss (tanδ) for various compositions of PNC nanocomposite films measured at 1kHz. Frequency dependence of (c) dielectric constant, (d) dielectric loss for PNC nanocomposites. It is interesting to note from Fig. 4.10 (b), that the dielectric loss (tanδ) for various compositions of PNC nanocomposite films are nearly comparable to that for pure PVDF film. Thus, the nanocomposite formation is significantly improving the dielectric constant without deteriorating the loss.

At room temperature and 1 kHz measuring frequency, dielectric permitivity of pure PVDF is 9, which increases significantly after PNC nanocomposite formation. The improvement in dielectric constant can be seen almost more than 200% for PVDF/N-CDs (1%) where it is 19.59. With decreasing N-CDs concentration in the PNC nanocomposite, the values of permittivity are lower viz. PVDF/N-CDs (1%) (19.59) > PVDF/N-CDs (0.5%) (15.22) >

PVDF/N-CDs (0.3%) (13.35) > pure PVDF (~9). The significant improvement in the dielectric permittivity of PNC nanocomposites can be attributed to the enhanced fraction of electroactive phases (β, γ-phase) in the nanocomposites and Maxwell-Wagner-Sillars type interfacial polarization contributions, which results due to the difference in conductivity and interfacial interaction between the PVDF and N-CDs. The PVDF is highly insulating while N-CDs are semiconducting[138,152]. Another reason could be the formation of micro capacitors in the nanocomposite films.[6,153] Thus, the synergetic effects from the surface functionality and high electroactivity of N-CDs has enhanced the dielectric constant of nanocomposite film[133].

Fig. 4.10(c), shows the frequency dependence of dielectric constant. The decrement in the dielectric constant with the increase in frequency is the evidence of interfacial polarization contribution. The interfacial polarization relaxation generates from the space charge and dipolar polarization relaxation at the nanocomposite interfaces[118,133]. Due to higher relaxation time, the space charge and dipolar polarization could not cope up with the electric field frequency variation, that results into the decrement of dielectric constant with the increasing frequency [118,133]. Fig. 4.10(d) shows the frequency dependence of dielectric loss. It is increasing with increasing frequency. The dielectric loss depends on the conduction loss of material and dielectric polarization loss mainly space charge migration and molecular dipoles movements. At the higher frequencies, the space charge accumulation is higher which results in increment in dielectric loss as seen in the frequency range 10^3 to 10^6 Hz [118,154].

The dielectric constant and loss with varying temperature at various frequencies are plotted in Fig. 4.11 and 4.12. At 1kHz all the compositions show larger temperature dependence, while, it is small for the higher frequencies. This clearly demonstrates interfacial polarization contributions in the response of developed PNC nanocapacitors films.

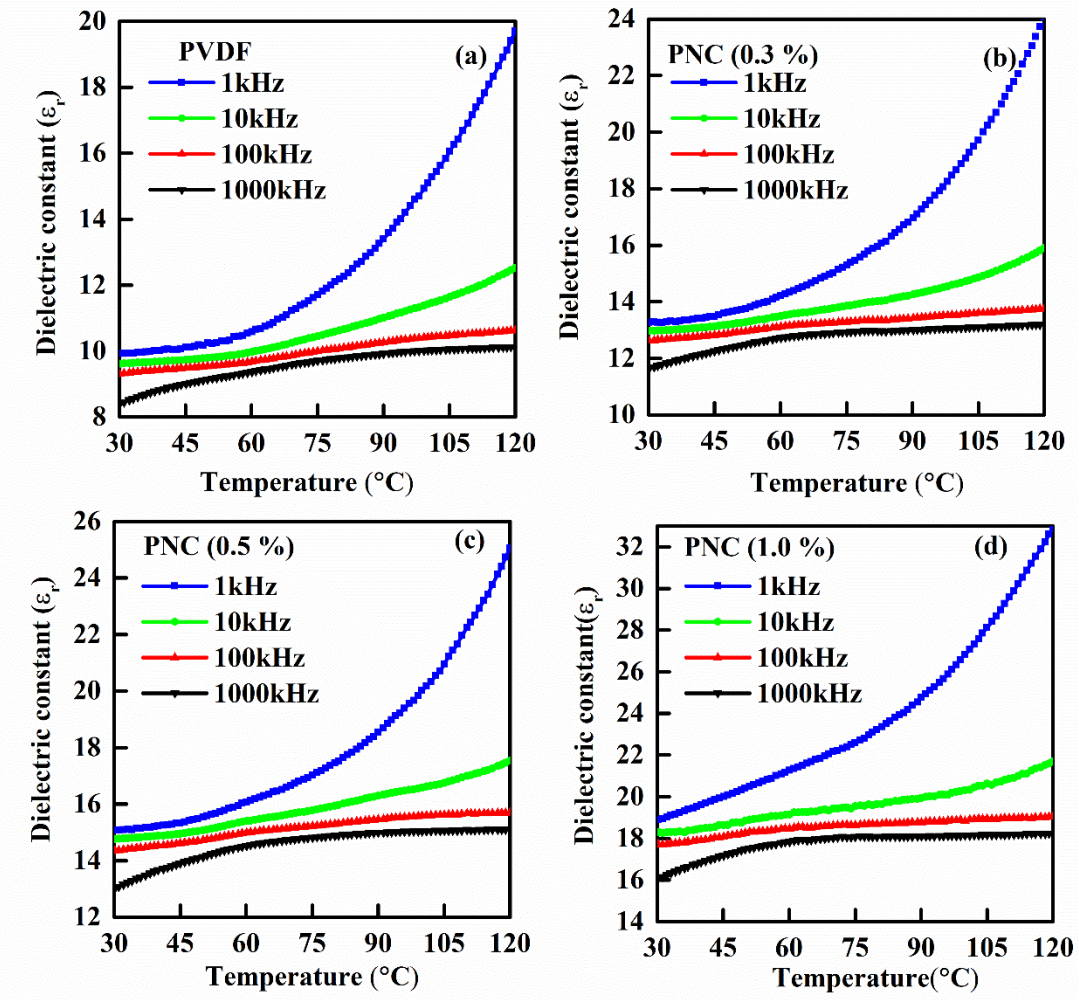

Figure 4.11 Temperature dependence of dielectric constant for (a) PVDF, (b) PNC (0.3%), (c) PNC (0.5%), (d) PNC (1.0%) films measured at various frequencies.

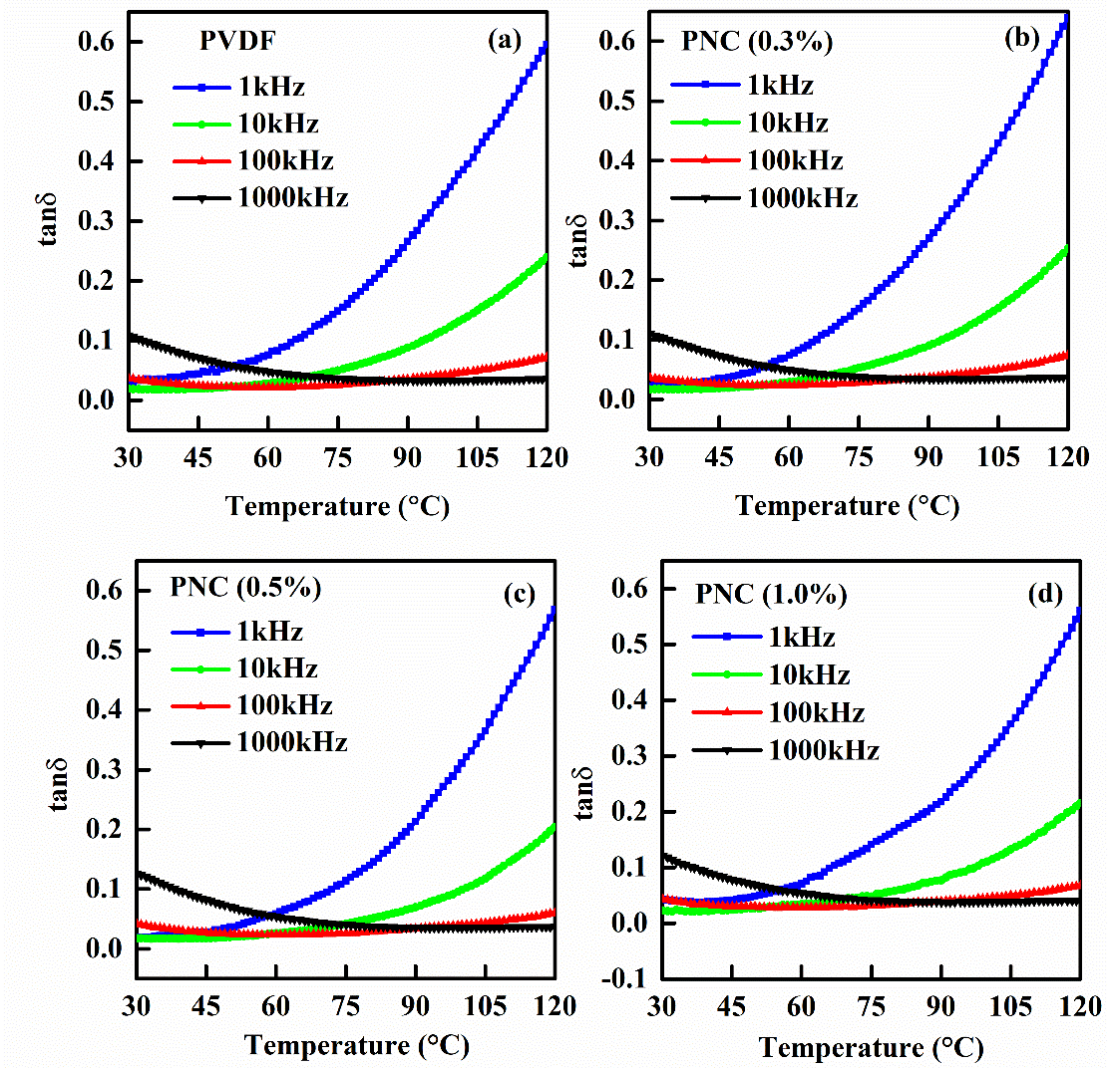

Figure 4.12 Temperature dependence of dielectric loss for (e) PVDF, (f) PNC (0.3%), (g) PNC (0.5%) and (h) PNC (1.0%) films measured at various frequencies.

Fig. 4.13 shows the AC conductivity plots with temperature and frequency for pure PVDF and PNC nanocomposite films. The conductivity is calculated with the help of the equation given below.

$$\sigma = 2\pi f \varepsilon_0 \varepsilon_r \tan\delta \qquad (4.3)$$

Where ε_0, 'σ' and 'f' are the permittivity of the air, AC conductivity and frequency of the applied field, respectively. Variation of the conductivity is governed by the response of the PVDF matrix at lower temperature but at higher temperature, the conductivity will be decided by the

semiconducting N-CDs response and the filler concentration. As can be seen from Fig.4.13 (a), the conductivity is higher at higher temperatures as well as for higher N-CDs filler concentration. At higher temperature, the conductivity of semiconducting materials increases due to the increasing numbers of conducting species in N-CDs. As shown in Fig. 4.13(b), the ac-conductivity of the various compositions of PNC nanocomposites are comparable to pure PVDF film up to 10^5 frequencies. It shows some dispersion at further higher frequencies. The higher filler concentration is having higher conductivity.

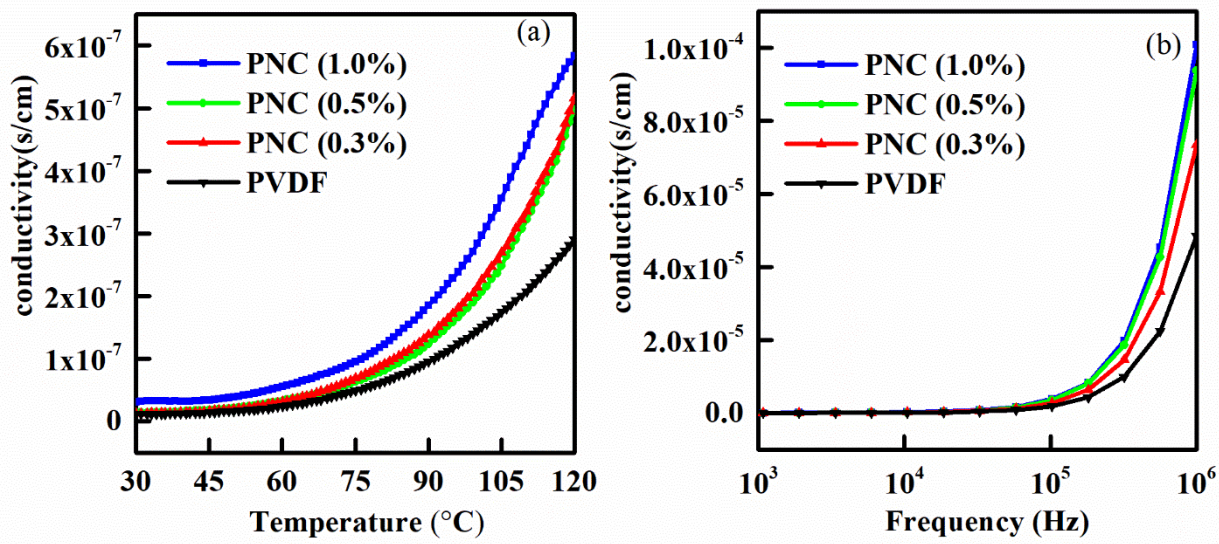

Figure 4.13 AC conductivity for the nanocomposite films with varying (a) Temperature, (b) Frequency.

6.3.7 Breakdown strength, P-E Hysteresis Loop and energy storage density

The electric breakdown strength of the developed PNC nanocomposites was characterized with the help of the ac- electrical breakdown strength test setup under the transformer oil environment. For the better estimate of the final breakdown strength, the test was performed on 7 film samples of each composition. The breakdown strength analysis is done with the help of the Weibull cumulative probability function as described in detail in chapter 1, equation (1.17) [51]. It can be expressed as,

$$P(E) = 1 - exp\left[-\left(\frac{E}{E_b}\right)^{\beta}\right]$$

where *P(E)* is the cumulative prospect of electrical breakdown, E is the actual breakdown field , E_b (kV/cm) is the breakdown field when the cumulative prospect is 63.2%, and β is the shape parameter obtained by linear fitting. A higher β value represents the better performance results in this analysis. We draw a plot between two parameters X_i, Y_i discussed in the equation (1.18), (1.19) of chapter 1 and given below as,

$$X_i = \ln (E_i)$$

$$Y_i = \ln \left[-\ln\left(1 - \frac{i}{n+1}\right)\right]$$

Where 'I' is the consecutive number of samples in 'n' numbers of samples, E_i is the experimentally measured value of applied electric field on samples.

Fig. 4.14(a) shows the Weibull analysis plots for the various compositions of PNC nanocomposites along with the pure PVDF film. The breakdown strength is seen to be slightly decreased as the nanofiller loading concentration is increased which is attributed to the presence of semiconducting N-CDs filler in the PVDF matrix increasing the chance of charge interference. The agglomeration of nanofillers in a particular region may also result in the charge accumulation and can lead to lowering of the breakdown strength of nanocomposites [58,156]. We have got better shape parameters for all the film samples as the value of β is quite high[155].

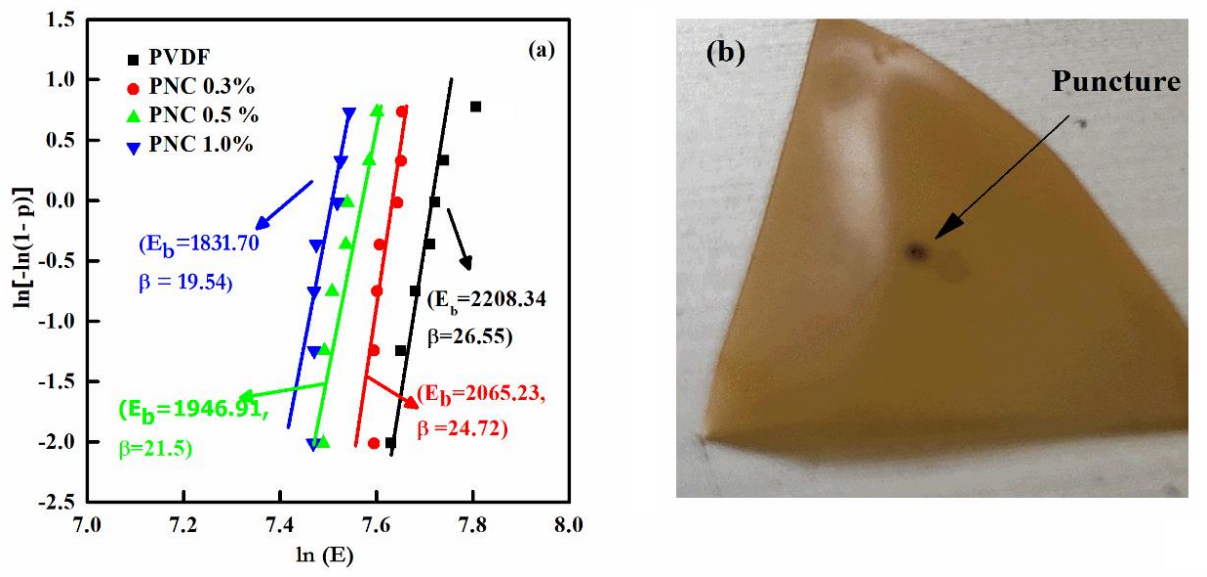

Figure 4.14 (a) Weibull analysis plot and (b) Sample image after breakdown showing puncture.

Fig. 4.14(b) shows a PNC nanocomposite film after breakdown puncture. Structural defects like pores can also be the reason for lowering the breakdown strength. The difference in the effective dielectric constant of PVDF and nanofiller creates an inhomogeneous electric field in the nanocomposite interfaces, which leads to a decrement in the breakdown strength, but due to the low amount of loading of nanofiller, the breakdown strength is still much better.

The breakdown strength of PVDF and its nanocomposite films calculated by Weibull probability analysis is used for finding the energy density using the equation (1.9) discussed in chapter 1 and given below,

where E_b is breakdown strength and ε_r is experimentally measured dielectric constant, this equation is accurately valid for the linear dielectric materials. However, as per the past practice in existing literature, it can be applied for comparative analysis of the different compositions even when the dielectric is slightly non-linear. The energy density determined for the PVDF/N-CDs (1%) is 2.89J/cm^3 which is much higher than the 1.94J/cm^3 for pure PVDF.

The Polarization(P)-Electric field(E) hysteresis loop can be used to analyze the non-linearlity in the dielectric response and the ferroelectric characteristics of the samples. Fig.

4.15(a) shows the half P-E hysteresis loops for the various compositions of the PNC nanocomposites and pure PVDF films, measured at room temperature, with applied electrical field up to 1500 kV at 25 Hz frequency. The measurement could not be performed at further, at higher electric fields due to the limitation of films thickness synthesized by the solution cast method and electric field supply of the instrument. The PVDF/N-CDs nanocomposites have significantly better polarization values than pure PVDF. The synergetic effects of the interfaces enhance the dielectric constant and polarization of the developed nanocomposites with conducting filler loading. Table 4.2 lists the values of measured polarization and energy storage parameters for various compositions of PNC and PVDF films. The resulting polarization response in nanocomposites is much higher than the pure PVDF film. This could be due to increased polar phase fraction and contributions coming from the interfacial polarization[138].

The discharged energy density was calculated using the ferroelectric loop for all the samples using the equation (1.11) discussed in chapter 1. Fig. 4.15(b) shows the discharged energy density for various compositions of PNC nanocomposites and the values are also listed Table 4.2. The value of discharged energy density calculated from P-E hysteresis loop measurements is not much less than that energy storage density, calculated from using the formula for the linear dielectrics, using Weibull analysis breakdown strength and the permittivity values. Table 4.2 shows the comparison between the energy densities calculated by the equations for the linear and nonlinear dielectrics. Since the P-E loop is not much non-linear for the investigated nanocomposite films samples, the difference between both the energy density values is small. The discharge energy efficiency (η) is calculated using the equation (1.13). The equations given for the energy storage density for linear system (U_e) (equation 1.9), discharge energy density (U_d) (equation 1.11), Energy loss (U_l) (equation 1.11) and discharge energy efficiency (η) (equation 1.13) are written below in respective manner.

Total energy storage density for linear system (U_e) = $\frac{1}{2}\varepsilon\varepsilon E_b^2$

Discharge energy density (nonlinear) (U_d) = $\int_{P_r}^{P_{max}} Edp$

Energy loss (U_l) = $\int_{0}^{P_{max}} Edp \; - \; U_d$

discharge energy efficiency (η) = $\frac{U_d}{U_d + U_{loss}}$

Where E is the applied electric field and P is the polarization, P_{max} is the maximum polarization with respect to maximum experimentally applied electrical field and P_r is the remanent polarization.

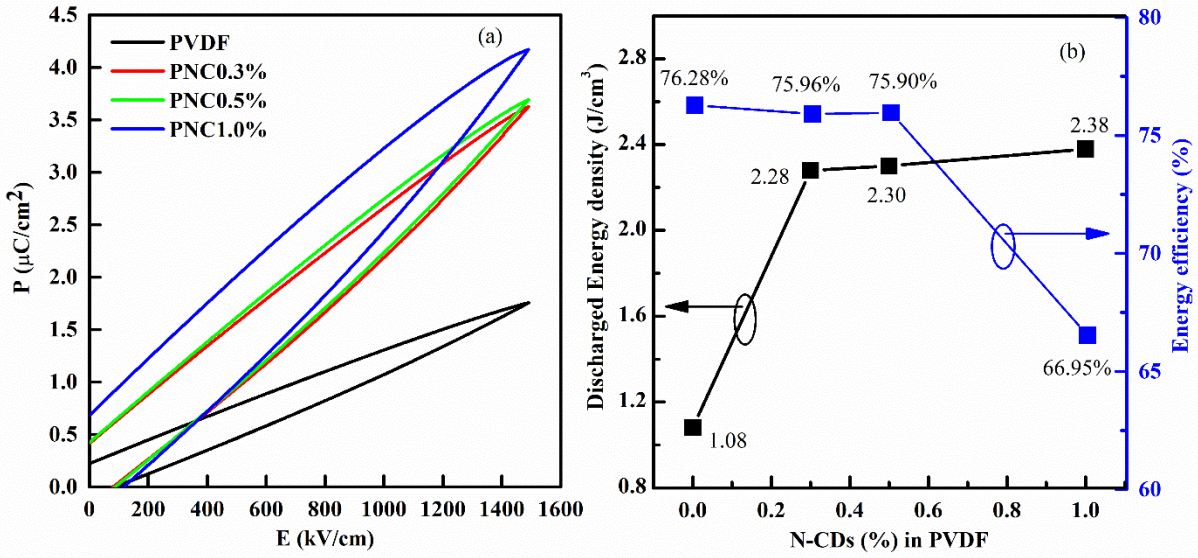

Figure 4.15 (a) P-E hysteresis loop at 25Hz and (b) Discharge energy density and discharge energy efficiency for pure PVDF and PNC nanocomposite films.

Table 4.2. P_r and P_{max} of PVDF and PVDF/N-CDs nanocomposite films and Energy density comparison calculated from different equations.

Sample	P_r ($\mu C/cm^2$)	P_{max} ($\mu C/cm^2$)	Total Energy density (U_e) (J/cm^3) = $\frac{1}{2}\varepsilon E_b^2$	Discharged Energy density (U_d) (J/cm^3) = $\int_{P_r}^{P_{max}} EdP$
Pure PVDF	0.33	1.79	1.94	1.08
PVDF/N-CDs (0.3%)	0.41	3.62	2.50	2.28
PVDF/N-CDs (0.5%)	0.42	3.69	2.54	2.30
PVDF/N-CDs (1.0%)	0.68	4.168	2.89	2.38

To analyze and visualize the electrical behaviour of the PNC nanocomposite films under external electrical field, the 2D simulation using finite element analysis (FEA) was carried out with the help of COMSOL Multiphysics 5.5. The dielectric constant of the N-CDs was determined using impedance spectroscopy, as shown schematically in Fig.4.16(a), and it was found to be 2.6. In simulated model of nanocomposite films, the nanofiller particles were dispersed randomly in the PVDF matrix as shown in Fig. 4.16(b). The dielectric constant for the PVDF matrix was taken to be 9. The 2D simulation results for current density, polarization, and electric field norm are shown in Fig. 4.16(c), (d) and (e), respectively. We can see that the filler particles are surrounded by more charge and conducting paths seem to be connected horizontally, but not vertically, which means filler particles are acting as micro-capacitors in this direction. If voltage is applied higher than the breakdown strength, then these conducting paths become more severe and pass the charge from one electrode to another, which results in the breakdown of the nanocomposite film. Polarization results shown in Fig. 4.16(d) demonstrates that the space charge polarization has played important role in enhancing the ferroelectric and dielectric properties in the nanocomposite films.

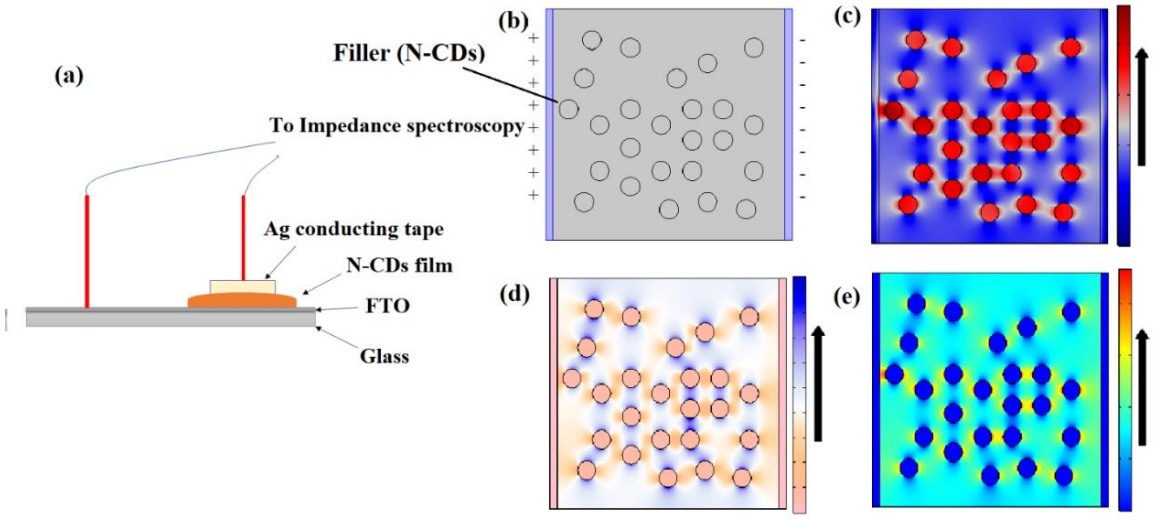

Figure 4.16 (a) Schematic diagram of dielectric constant measurement of N-CDs, (b) 2D Schematics of PVDF/N-CDs film, (c) Current density norm, (d) Polarization and (e) Electric field distribution.

The enhancement in the energy density of the PNC nanocomposite films and appropriate discharge efficiency of the PNC nanocomposite films make them suitable for the high capacitive energy density storage applications. A comparison of our results with the existing literature for the dielectric constant, discharge energy density and storage efficiency for different nanocomposite films at given applied electric field is listed in Table 4.3. It shows that the performance of PVDF/N-CDs nanocomposite films developed in the present work is quite better for the capacitive energy storage applications.

Table 4.3. A comparison of the dielectric constant, discharge energy density and discharge efficiency at the given applied electric field for different nanocomposite films.

Sample	U_d (J/cm^3)	(η%)	E (kV/cm)	ε_r	Reference
PVDF/Fe-rGO (3%wt)	1.45	62	550	57	[157]
PVDF/TiO_x (1%wt)	4.08 (7.43*0.55)	~55	4800	22	[10]
PVDF/MXene (1%wt)	4.57	43.83	2250	18	[158]

Epoxy/h-BN-rGO (26.0%Vol)	0.51	77.0	1000	~11	[127]
PVDF/rGO-Ag (1%wt)	0.26	--	150	-	[128]
PVDF/N-CDs (1%wt)	2.38	66.95	1500	19.59	This work

6.4 Theoretical analysis of percolation and interface thickness

We have discussed in section 1.4 of chapter 1 about interface thickness and inter-filler distance effects in nanocomposite dielectric films. The interface formation take place when different fermi level energies are there for the filler and matrix materials. This interface effect is due to the Gouy chapman stern layer that's called as diffuse layer as well. The N-CDs are the semiconducting filler, have band gap of 3.0eV with a diameter size of 2.44nm as evidenced from the HRTEM micrographs shown in the Fig. 4.2 (a). The charge density of the N-CDs is ~$1.9 \times 10^{17}/cm^3$ as reported in earlier literature [137,159]. The dielectric constant for N-CDs is ~2.6. The Debye length for the interface in the nanocomposite film calculated from the equation (1.15) is obtained to be ~4.5nm. Further, the inter-filler distance (δ_i) calculated with the help of equation (1.16), for the PNC 1wt% comes out to be ~6.5nm and for PNC 2wt%; it is ~4.5. Thus, the Inter-filler distance for the 2wt% is almost equal to the Debye length of the N-CDs loaded in the PVDF. This suggest that the performance of the nanocomposite films will be compromised for filler loading more than 2wt.% as already discussed in Chapter 1. In view of this, we have performed the P-E hysteresis loop analysis on PVDF/N-CDs (2wt%) composition and the results are shown in the Fig. 4.17. The breakdown of the nanocomposite films was at lower value as evidenced by the Fig. 4.17 and the polarization value is lower as well. The lossy curve can be seen in the Fig. 4.17.

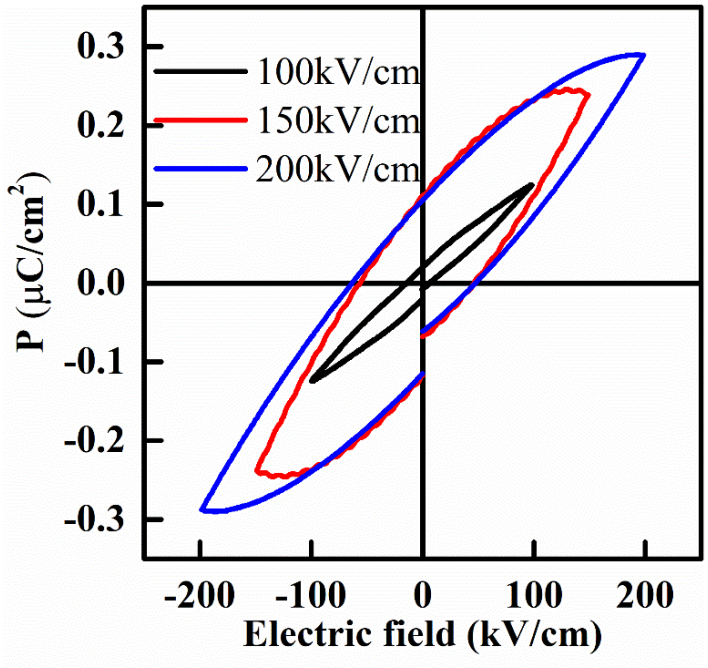

Figure 4.17 Hysteresis loop of PVDF/N-CDs (2wt%) measured at 10Hz.

6.5 Conclusions

A facile synthesis of PVDF/N-CDs nanocomposite films is demonstrated with effective strategy for enhancement of the dielectric and ferroelectric properties to use in capacitive energy storage devices. The N-CDs were synthesized using Solvothermal process and characterized using HR-TEM to know the size distribution. The band gap of N-CDs was calculated using Tauc's plot from UV-Vis. spectroscopy. Loading of N-CDs as filler in PVDF matrix enhanced the formation of polar β-phase of PVDF which resulted in increment in the dielectric constant, polarization and energy storage density of nanocomposites. The Weibull probability analysis is done to calculate the most appropriate dielectric breakdown strength of all the developed nanocomposite films including neat PVDF. The significant improvement in the dielectric constant (ε_r =19.59) and discharge energy density (U_d =2.38J/cm^3) is demonstrated with the 1% loading of the N-CDs as filler.

On the basis of the results and findings in this chapter, we have filed an Indian patent on 26/08/2022 with Application No. 202211048961, It has been published on 23/12/2022 on the OFFICIAL JOURNAL OF THE PATENT OFFICE, Indian Patent office, New Delhi